Homogenization of Form-Wound Windings in Frequency and Time Domain Finite Element Modelling of Electrical Machines

Johan Gyselinck [1], Patrick Dular [2,3], Nelson Sadowski [4], Patrick Kuo-Peng [4], Ruth V. Sabariego [2]

[1] Dept. of Bio-, Electro- and Mechanical Systems (BEAMS), Université Libre de Bruxelles (ULB), Belgium
[2] Dept. of Electrical Engineering and Computer Science (ACE), University of Liège, Belgium
[3] Fonds de la Recherche Scientifique, F.R.S. – FNRS, Belgium
[4] GRUCAD/EEL/CTC, Universidade Federal de Santa Catarina, Brazil

In this paper the authors deal with the FE modelling of eddy-current effects in form-wound windings of electrical machines using a previously proposed general frequency and time domain homogenization method. By way of demonstration and validation, a real-life 1250 kW induction machine with double-layer stator winding is considered. The skin and proximity effects in one stator conductor (copper bar) are first quantified by means of a simple low-cost FE model, leading to complex and frequency-dependent coefficients for the homogenized winding (reluctivity for proximity effect and conductivity or resistance for skin effect). These complex coefficients are subsequently translated into real-valued and constant coefficients that allow for time-domain homogenization when introducing a limited numer of additional degrees of freedom in the FE model. All results obtained with the homogenized model (considering one conductor or a complete slot) agree well with those produced by a brute-force approach (modelling and finely discretizing each conductor).

Index Terms— **Finite element methods, magnetic fields, time and frequency domain, homogenization, electrical machine, windings**

I. Introduction

Multi-turn windings in electromagnetic devices may be subjected to considerable skin and proximity effects, leading to higher losses and hot spots, and possibly affecting the global characteristics of the device. In principle these effects can be taken into account in a FE simulation of the device by modelling and finely discretising each separate conductor (with additional electrical circuit equations to connect the so-called massive conductors [1]). For most real-life applications the huge computational cost of such a brute-force approach cannot be justified. Most often the eddy-current effects are thus simply ignored in the resolution stage of the FE simulation (considering winding regions with uniform current density, so-called stranded conductors [1]). In this case the eddy-current losses may be estimated *a posteriori*.

Frequency-domain homogenization methods for windings have recently been proposed in [2][3]. For the winding type in hand (e.g., round wires with hexagonal-like packing or rectangular conductors with rectangular packing), an elementary FE model is used for determining frequency-domain coefficients regarding skin and proximity effect [3]. These frequency-dependent coefficients can next be straightforwardly translated into constant time-domain coefficients and associated differential equations thanks to the introduction of a limited number of additional unknowns for the homogenized winding (current components for the skin effect, and induction components for the proximity effect) [4]. The number of additional unknowns required and the additional computational cost depend on the frequency content of the application and in particular on the conductor size (e.g. radius in case of conductors of circular cross-section) to skin depth ratio (considering the highest relevant frequency).

So far the abovementioned frequency and time domain homogenization methods have been mainly applied to inductor-like devices, having a multi-turn multi-layer winding, and in which a 2-D flux pattern produces the dominant proximity effect [3], [4]. In this paper we consider a 1250 kW induction machine and in particular its form-wound stator winding [5][6]. Compared to previous applications, the flux situation is *a priori* simpler, the slot leakage flux being essentially governed by a 1-D differential equation and allowing for an approximate analytical approach.

However, when conductors are connected in parallel, with furthermore transposition from one slot to the next, as it is the case in the considered induction machine, the homogenization of the winding, following a general approach, is less straightforward.

We therefore focus in this paper on the time and frequency domain homogenization of the winding while assuming a simple series connection of all conductors. This allows to consider only one conductor (for determining the homogenization coefficients) and subsequently one slot. A brief discussion on the possible parallel connection and transposition of the conductors follows.

Manuscript received December 23, 2009. Corresponding author: J. Gyselinck (e-mail: johan.gyselinck@ulb.ac.be).

II. Geometry of stator slots and conductors

Figure 1 shows the geometry of the 50 Hz 1250 kW three-phase six-pole squirrel-cage induction machine [5]. The two-layer stator winding of the machine is distributed in 72 rectangular and fully-open slots (slot width $w_s = 14$ mm, total slot height 80 mm), each slot comprising 2×9 copper bars of rectangular cross-section (conductor height $h_c = 3.3$ mm, conductor width $w_c = 10.6$ mm) [5].

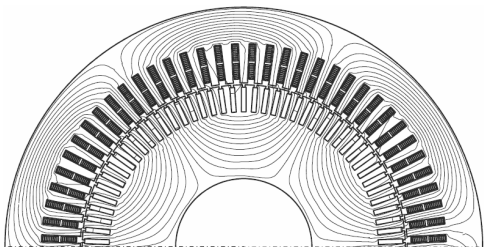

Fig. 1. 2D FE model of 1250 kW induction motor (half cross-section) [6]

The vertical insulation space between two conductors of the same group is $h_i = 0.5$ mm, while the two groups of conductors are separated by 4.9 mm (see Fig. 2). The lamination stack length is $l = 810$ mm.

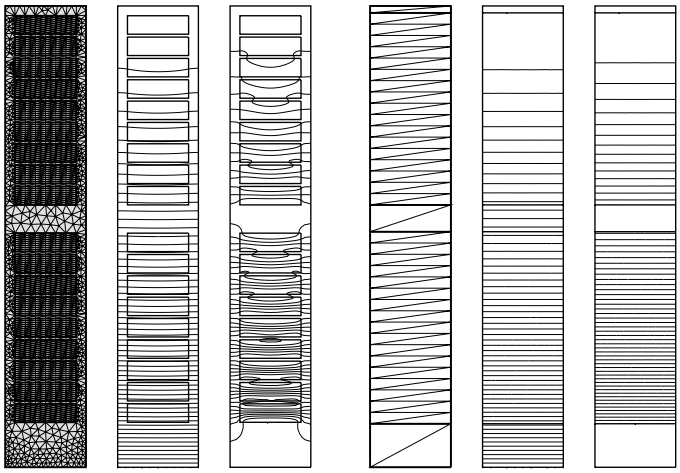

Fig. 2. FE mesh and flux lines (flux component in phase and in quadrature, respectively, with the same imposed 50 Hz current in all 18 conductors), fine model (for brute-force approach) and homogenized model

Flux and current harmonics in the machine are due to the stator and rotor slotting, saturation and PWM supply (at 2 kHz switching frequency) [6].

Taking as conductivity $\sigma = 6 \cdot 10^7$ S/m, the skin depth $\delta = \sqrt{2/(\omega\mu\sigma)}$, at pulsation ω, varies between 9.2 mm (at 50 Hz) and 1.45 mm (at 2 kHz), and the conductor height to skin depth ratio, h_c/δ, between 0.35 and 2.27.

III. Skin and proximity effect in one conductor

A. Elementary FE model and frequency-domain calculations

We consider an elementary FE model comprising one copper bar (modelled as a massive conductor) and the insulating space around it. Frequency-domain calculations are carried out in terms of the complex single-component magnetic vector potential $\boldsymbol{a}$ (in bold), with adequate current and boundary conditions [1].

The complex power $\boldsymbol{S}$ (in volt-ampères) is calculated from the local flux density $\boldsymbol{b}$ and the local current density $\boldsymbol{j}$:

$$\boldsymbol{S} \;=\; P + \imath\, Q \;=\; \frac{l}{2} \int_\Omega (j^2/\sigma + \imath\, \omega\, \nu_0\, b^2)\, d\Omega\,, \qquad (1)$$

with P and Q the active and reactive power (averaged over a fundamental period), $\imath$ the imaginary unit, and $j^2/2 = \boldsymbol{j}\boldsymbol{j}^*/2$ and $b^2/2 = \boldsymbol{b}\boldsymbol{b}^*/2$ r.m.s.-values squared.

Equation (1) can be rewritten considering the average current density $\boldsymbol{j}_{av}$ and flux density $\boldsymbol{b}_{av}$ (averaged over the complete elementary model, i.e. copper plus insulation):

$$\boldsymbol{S} \;=\; \frac{l}{2} \int_\Omega (j_{av}^2/\boldsymbol{\sigma}_{skin} + \imath\, \omega\, \boldsymbol{\nu}_{prox}\, b_{av}^2)\, d\Omega\,, \qquad (2)$$

and we thus define the complex skin-effect conductivity $\boldsymbol{\sigma}_{skin}$ and the complex proximity-effect reluctivity $\boldsymbol{\nu}_{prox}$.

B. Skin effect

Following the approach developed in [3], [4], a pure skin-effect excitation is obtained by imposing a sinusoidal current (of unit amplitude, e.g., $I = 1$) in the bar, with condition $\boldsymbol{a} = 0$ on the complete boundary (effecting $b_{av} = 0$). See the flux patterns in Fig. 3.

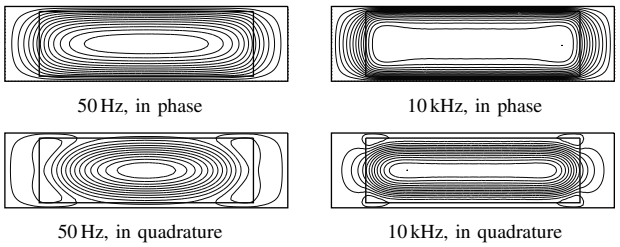

Fig. 3. Skin-effect flux pattern at 50 Hz and 10 kHz, with flux component in phase and in quadrature with the imposed net current

The joule losses at frequency f (current amplitude I) and under DC conditions (constant current I and uniform current density, i.e. no skin effect) can be expressed as $P = R_{AC} I^2/2$ and $P = R_{DC} I^2$, respectively. Fig. 4 shows the ratio R_{AC}/R_{DC} as a function of h_c/δ, obtained with the elementary FE model. This figure also shows the analytical approximation which is based on the 1D diffusion problem (net current, or alternatively net flux, in a conducting sheet of thickness h_c) [7]:

$$\frac{R_{AC}}{R_{DC}} = \Re(\boldsymbol{Y})\,, \qquad (3)$$

where the complex number $\boldsymbol{Y}$ is a function of h_c/δ:

$$\boldsymbol{Y} \;=\; \frac{1+\imath}{2}\, \frac{h_c}{\delta}\, \operatorname{cotanh}\Big(\frac{1+\imath}{2}\, \frac{h_c}{\delta} \Big)\,. \qquad (4)$$

The analytical solution is apparently valid up to, say, h_c/δ equal to 2. The relative increase in joule losses due to skin effect, i.e. the ratio R_{AC}/R_{DC} minus 1, is found to vary between 0.01% at 50 Hz ($h_c/\delta = 0.35$) and 12% at 2 kHz ($h_c/\delta = 2.27$).

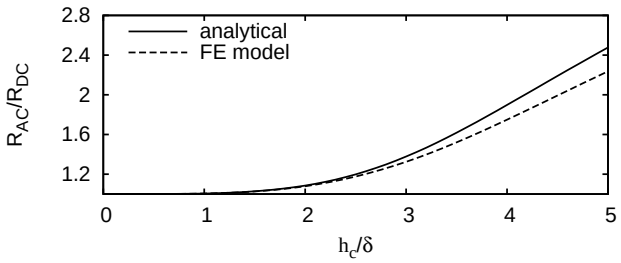

Fig. 4. Ratio R_{AC}/R_{DC} as a function of h_c/δ, obtained analytically and with the elementary FE model

C. Proximity effect in frequency domain

A pure proximity-effect excitation is obtained by imposing a unit horizontal flux (with $\boldsymbol{a} = 0$ and $\boldsymbol{a} = 1$ on lower and upper boundaries, respectively, and the implicit Neumann condition $\partial a/\partial n = 0$ on left and right slot walls) and zero net current ($I = 0$). See the flux patterns in Fig. 5.

The complex proximity-effect reluctivity $\boldsymbol{\nu}_{prox}$ can also be estimated on the basis of the same well-known analytical solution (4) of the 1D diffusion problem and considering the flux tubes connected in series (left and right) and in parallel (up and down) with the copper bar:

$$\boldsymbol{\nu}_{prox} \;=\; \nu_0 \, \Big(\Big(\frac{w_c}{h_c}\, \boldsymbol{Y} + \frac{w_s - w_c}{h_c} \Big)^{-1} + \frac{h_i}{w_s} \Big)^{-1}\,. \qquad (5)$$

Fig. 6 shows the relative proximity-effect reluctivity $\boldsymbol{\nu}_{prox}/\nu_0$ as a function of h_c/δ, obtained in three different

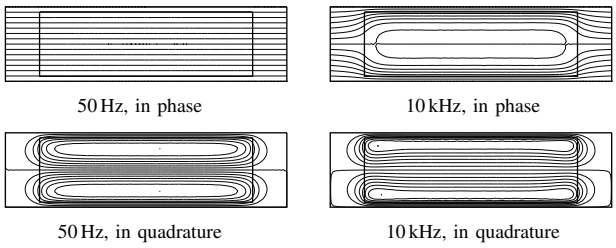

Fig. 5. Proximity-effect flux pattern at 50 Hz and 10 kHz, with flux component in phase and in quadrature with the imposed flux

ways: first considering the complex number $\boldsymbol{Y}$ (i.e. without any consideration for the space around the bar), second adopting (5), and third using the elementary FE model. Clearly, the correction for the insulation on all four sides of the conductor is required for getting a good accuracy in the considered h_c/δ range.

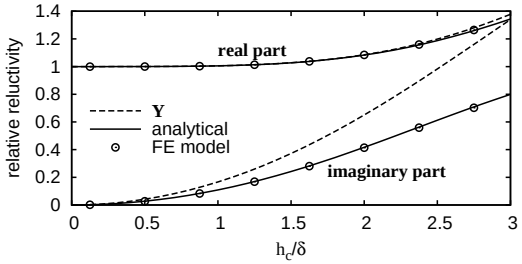

Fig. 6. Real and imaginary part of the relative permeability $\boldsymbol{\nu}_{prox}/\nu_0$ versus h_c/δ, obtained with the elementary FE model and using analytical formulas

D. Proximity effect in time domain

The frequency-dependent reluctivity $\boldsymbol{\nu}_{prox}(h_c/\delta)$ can be translated in an equivalent time-domain relation between the instantaneous magnetic field $h(t)$ and the magnetic flux density $b(t)$ by considering $n-1$ auxiliary flux density components $b_2(t)$, $b_3(t)$, ..., $b_n(t)$ [4]. A system of n first-order differential equations can then be written in terms of the column matrices $[B(t)]^T = [b(t)\ b_2(t)\ b_3(t)\ \ldots]^T$ and $[H(t)]^T = [h(t)\ 0\ 0\ \ldots]^T$:

$$[H(t)] \;=\; \nu_0 \left([B(t)] + \frac{\sigma \mu_0 h_c^2}{4} [\mathcal{P}^{(n)}] \frac{d}{dt} [B(t)] \right) , \qquad (6)$$

where $[\mathcal{P}^{(n)}]$ is a real-valued, dimensionless, symmetric and tridiagonal matrix.

In the frequency domain (6) becomes

$$[\boldsymbol{H}] \;=\; \nu_0 \left([1] + \boldsymbol{\imath}\, \sigma \frac{h_c^2}{2} [\mathcal{P}^{(n)}] \right) [\boldsymbol{B}] , \qquad (7)$$

with $[1]$ the $n \times n$ identity matrix, from which the approximate complex reluctivity $\boldsymbol{\nu}_{prox,n}(h_c/\delta)$ can be readily calculated. By properly fitting the elements of $[\mathcal{P}^{(n)}]$, with a sufficiently great value for n, a good agreement between $\boldsymbol{\nu}_{prox,n}(h_c/\delta)$ and $\boldsymbol{\nu}_{prox}(h_c/\delta)$ can be obtained up to a preset value of h_c/δ.

With $n = 3$ the following values are obtained through fitting:

$$[\mathcal{P}^{(3)}] = \begin{bmatrix} 0.1085 & 0.0747 & 0 \\ 0.0747 & 0.0596 & 0.0103 \\ 0 & 0.0103 & 0.0166 \end{bmatrix} , \qquad (8)$$

Figure 7 shows that with $n = 2$ an excellent agreement is obtained up to $h_c/\delta = 4$. The approximation with $n = 1$ is valid up to, say, $h_c/\delta = 1$.

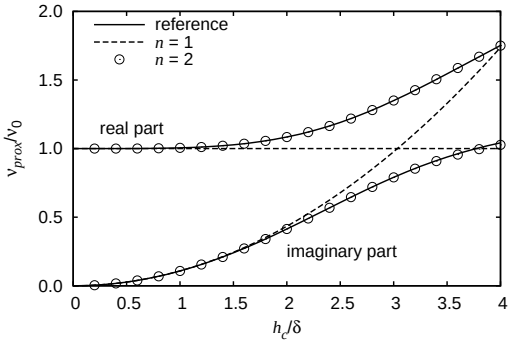

Fig. 7. Real and imaginary part of the relative permeability $\boldsymbol{\nu}_{prox}/\nu_0$ versus h_c/δ, obtained directly in the frequency domain (reference) and indirectly in the time domain (with fitted $[\mathcal{P}^{(1)}]$ and $[\mathcal{P}^{(2)}]$)

The integration of the additional flux density components in the FE equations is developed in [4].

IV. Homogenization of a complete slot

We now carry out time and frequency domain calculations using a FE model of a complete slot, with either a fine discretisation of each conductor (18 massive conductors) or homogenization of the two groups of nine conductors each (two stranded conductors). The two meshes used (totaling 3618 first-order triangular elements versus 74) are represented in Fig. 2. All nine conductors in a group are assumed connected in series.

A. Frequency domain

The complex reluctivity $\boldsymbol{\nu}_{prox}$ is adopted in the two homogenized winding regions, together with an imposed uniform current density. The equivalent AC resistance R_{AC} is to be used in the electrical-circuit equations (if any).

Two cases are further considered, the two conductor groups belonging either to the same phase or to different phases, and with either zero or 120 degree phase shift between the respective currents (of same unit amplitude, $I = 1$). Some flux patterns (with all conductors belonging to the same phase) are depicted in Fig. 2.

Using (1) and (2) we obtain the complex power and thus the equivalent AC resistance $R_{AC} = P/(2I^2)$ and AC inductance $L_{AC} = Q/(2\omega I^2)$ at a given pulsation ω. Fig. 8 shows the ratios R_{AC}/R_{DC} and L_{AC}/L_{DC} as a function of h_c/δ. There is an excellent agreement between the results obtained with the brute-force approach and with the homogenized model.

For the one-phase case, e.g., at 50 Hz the resistance increases by 34%, and at 2 kHz by a factor of 300. Clearly, the skin-effect losses are negligible compared to the proximity-effect losses (considering the 0.01% and 12% increases mentioned above).

B. Time domain

The current waveform considered for the time-domain calculations (current imposed in all 18 conductors) is depicted in Figure 9. The main frequency components are the 50 Hz fundamental (amplitude 313.2 A) and the 1850 Hz and 2050 Hz

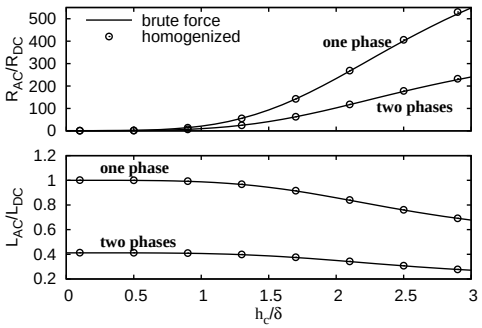

Fig. 8. Relative AC resistance and inductance (with DC values as reference) versus h_c/δ for a complete slot, obtained with reference FE model (brute force approach) and with homogenized FE model

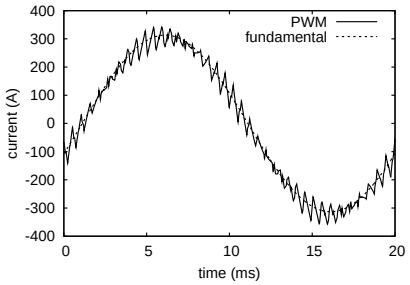

Fig. 9. PWM waveform of the imposed 50 Hz current

switching harmonics (19.5 A et 17.6 A, respectively). This current waveform is similar to the currents shown in [5][6].

Figure 10 depicts the instantaneous joule losses in the slot (18 conductors) during 3 ms (i.e. approximately 6 PWM switching periods). The homogenization with $n = 1$ is clearly much less accurate than the one with $n = 2$.

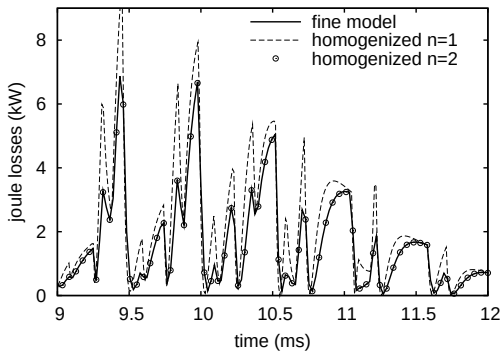

Fig. 10. Instantaneous joule losses in slot calculated with fine FE model and homogenized FE model

V. Parallel connection and transposition

The stator winding of the considered machine comprises three parallel branches [6]. This means that a group of nine conductors in a slot constitutes three effective turns with another group of nine conductors in another slot (5/6 of a pole pitch away in this case). As the machine has four slots per pole and per phase, the conductors are transposed in order to reduce effectively the unequal distribution of the current among the three parallel paths. FE simulation of the complete machine shows that circulating circuits are practically zero thanks to the transposition [6]. This means that each of the nine bars in a group carries the same current, as assumed in the above sections.

Figure 11 shows the effect of the parallel paths inside a single slot (one-phase case), disregarding the transposition from one slot to the next. However, transposition inside the two halfs of one slot is possible and clearly reduces the circulating currents (ABC/CAB versus ABC/ABC).

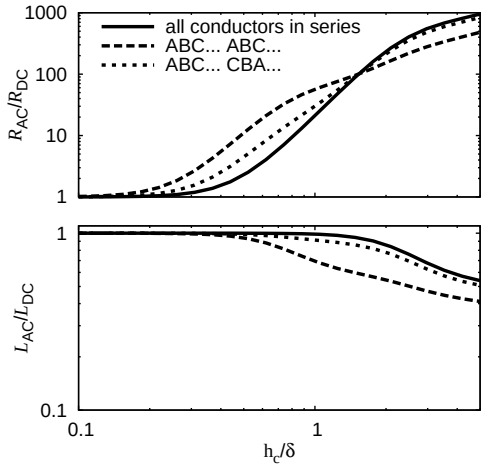

Fig. 11. Effect on resistance and inductance of the three parallel paths in a single slot (considering the transposition among the two groups or not)

VI. Conclusion

Frequency and time domain homogenization methods have been successfully applied to the form-wound winding of an induction machine, hereby assuming a plain series connection of the copper bars and disregarding their actual transposition in the slots. Thanks to the transposition, circulating currents are very small, so that the simplified analysis carried out is also relevant for the real winding (with transposition). In case of PWM supply, the homogenization method with one additional degree of freedom (i.e. $n = 2$) produces accurate results.

Acknowledgment

This work was partly supported by the Belgian Science Policy (IAP P6/21), the Belgian F.R.S.–FNRS and the Brazilian CNPq.

References

[1] P. Lombard and G. Meunier, "A general purpose method for electric and magnetic combined problems for 2D, axisymmetric and transient systems", *IEEE Trans. on Magn.*, vol. 29, pp. 1737–1740, March 1993.

[2] A. Podoltsev, I. Kucheryavaya, and B. Lebedev, "Analysis of effective resistance and eddy-current losses in multiturn winding of high-frequency magnetic components," *IEEE Trans. on Magn.*, vol. 39, pp. 539–548, January 2003.

[3] J. Gyselinck and P. Dular, "Frequency-domain homogenization of bundles of wires in 2D magnetodynamic FE calculations," *IEEE Trans. on Magn.*, vol. 41, pp. 1416–1419, April 2005.

[4] J. Gyselinck, R. Sabariego, and P. Dular, "Time-domain homogenisation of windings in two-dimensional finite element models", *IEEE Trans. on Magn.*, vol. 43, pp. 1297–1300, 2007.

[5] M. Islam and A. Arkkio, "Effects of pulse-width-modulated supply voltage on eddy currents in the form-wound stator winding of a cage induction motor," *IET Electr. Power Appl.*, vol. 3, pp. 50–58, 2009.

[6] M. Islam, "Finite-element analysis of eddy currents in the form-wound multi-conductor windings of electrical machines," PhD thesis, Helsinki University of Technology, to be published in 2010.

[7] J. Lammeraner and M. Stafl, "Eddy currents," London, U.K.: ILIFFE Books, 1966.